REVIEW OF SCIENTIFIC INSTRUMENTS **88**, 053904 (2017)

Transient surface photovoltage measurement over 12 orders of magnitude in time

Thomas Dittrich,[1] Steffen Fengler,[2] and Michael Franke[3]
[1]*Helmholtz-Zentrum Berlin für Materialien und Energie GmbH, Institut für Silizium-Photovoltaik, Kekuléstr. 5, D-12489 Berlin, Germany*
[2]*Helmut-Schmidt-Universität, Institut für Werkstofftechnik, Holstenhofweg 85, D-22043 Hamburg, Germany*
[3]*Elektronik-Manufaktur Mahlsdorf, Paul-Wegener-Str. 36, D-12623 Berlin, Germany*

(Received 16 December 2016; accepted 20 April 2017; published online 19 May 2017)

The measurement of transient surface photovoltage (SPV) signals in a fixed capacitor arrangement over 12 orders of magnitude in time has been demonstrated for a SnO_2:F/TiO_2/In_2S_3 layer system under high vacuum. For this purpose, a high impedance buffer with a bandwidth above 200 MHz and an effective input resistance of 200-700 TΩ has been developed. Fast separation of photo generated charge carriers within ns and very slow relaxation of SPV signals excited with short laser pulses and the measurement of SPV spectra under continuous illumination with a halogen lamp were demonstrated. *Published by AIP Publishing.* [http://dx.doi.org/10.1063/1.4983079]

I. INTRODUCTION

Separation of photo generated charge carriers in space is key for many applications such as in photovoltaics or in photocatalysis. In solar cells as well as in photocatalysts, processes of photo-generation, charge separation, charge transport, trapping, and recombination play an important role for the performance of related devices. Surface photovoltage (SPV) techniques allow for the investigation of processes in photoactive materials and can therefore contribute to a further improvement of understanding of photoactive materials and therefore also to an improvement of the performance of solar cells and photocatalysts. It is of great interest to extend the time range of SPV measurements towards both short and long times for getting a deeper understanding of the hierarchy of photo-electric and photo-chemical processes in photoactive materials.

A surface photovoltage is defined as the negative change in the contact potential difference (CPD) of a sample under illumination.[1] There are different ways to measure the light induced change of CPD (ΔCPD) which are shown schematically in Figure 1. The most fundamental way is the use of a Kelvin-probe[2] consisting, for example, of a vibrating gold mesh (reference electrode), a dc voltage source, and a lock-in amplifier for measuring the ac current. In the Kelvin-probe, the ac current is adjusted to zero by changing the dc voltage so that the difference of the CPD at the surface of the sample and of the CPD at the surface of the reference electrode is equal to the dc voltage. SPV signals can be measured with a Kelvin-probe under continuous illumination together with the variation of the wavelength (also known as SPS–surface photovoltage spectroscopy[1]). Typical resolution times are of the order of seconds for SPV measurements with a Kelvin-probe. In a Kelvin-probe force microscope (KPFM), the electrostatic force between the surface of the sample and the surface of the tip is minimized with an external voltage (CPD feedback[3]). A KPFM allows for SPV measurements with a high resolution in space, usually limited by the transport length of photo-generated minority charge carriers.[4] For highly sensitive spectral dependent quasi SPV measurements in ultra-high vacuum (UHV), the dc current of low energetic electrons can be adjusted to a constant value with an external voltage source (EB-SPV–electron beam SPV[5,6]). In SPV measurements with a Kelvin-probe, a KPFM and EB-SPV, the SPV signals are obtained by adjusting an ac current, an electrostatic force, or a dc current, respectively, to zero or to a constant value with an external voltage. This principle does not allow for fast SPV measurements.

A change of the CPD of a surface in UHV can also be detected from the shift of core levels in x-ray photoelectron spectroscopy (XPS). The shift of a core level can be caused by a surface photovoltage, i.e., XPS can be applied for the measurement of SPV signals (XPS-SPV).[7] However, x-rays and emitted photoelectrons may interact at or near the surface. In recent years, opportunities to apply short bunches of x-rays for time dependent probing of surfaces have been created at several synchrotron light sources, so that a sampling of XPS spectra became possible after the interaction with short laser pulses.[7–9] The time range of XPS-SPV depends on the sampling rate, averaging, and on the duration time and the repetition rate of the laser pulses.

Fast SPV measurements over a wide range in time can be easily performed only in the fixed capacitor arrangement in which a constant measurement capacitor is formed between the sample and a reference electrode. First transient SPV measurements were carried out at a resolution time of the order of μs (excitation with a spark gap).[10] Now, pulsed lasers and conventional electronics allow for detection of SPV signals with resolution times of the order of ns and even less. Transient SPV measurements over up to 7 orders of magnitude in time were shown.[11] However, these measurements were limited at longer times to about 0.1 s. In this work, we close the gap between transient SPV and SPV with a Kelvin-probe by extending the range of transient SPV measurements to 12 orders of magnitude in time. For this purpose, a suitable high impedance buffer was developed and a sample with a SnO_2:F/TiO_2/In_2S_3

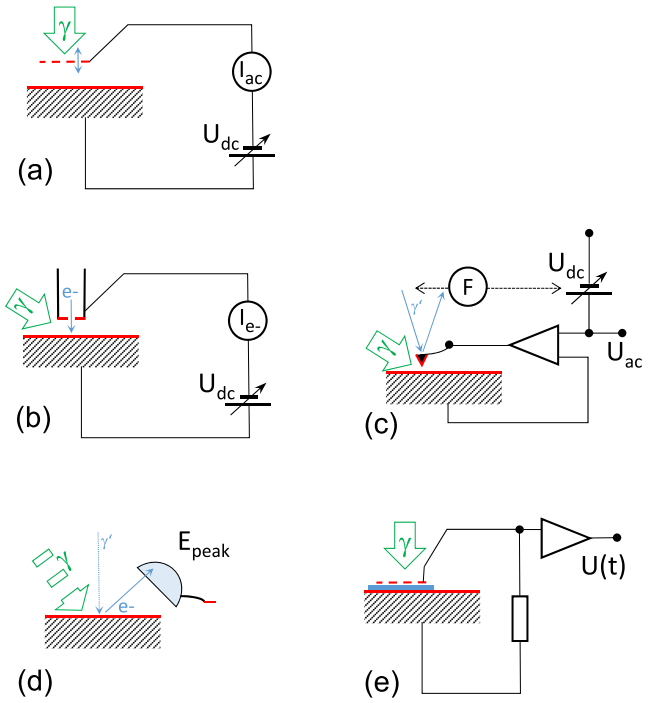

FIG. 1. Measurement principles of surface photovoltage signals: Kelvin-probe (a), electron beam current (b), Kelvin-probe force microscope (c), photoelectron spectroscopy (d), and fixed capacitor (e). In (a)-(c), the dc voltage is adjusted so that the ac current, the electron current, or the force are kept at zero, low, or minimum values, respectively. In (d), the light induced shift of core levels is measured. The time dependent SPV signal is directly measured only in (e).

layer system was chosen to demonstrate related transient and spectral dependent SPV measurements.

II. CRITICAL PARAMETERS IN TRANSIENT SURFACE PHOTOVOLTAGE MEASUREMENTS

In SPV measurements in the fixed capacitor arrangement, a light pulse interacts with a sample and the resulting separation of photo generated charge carriers leads to charging of the measurement capacitor (C_m, see Figure 2). The change of the corresponding electric potential across the capacitor (U_{in}) is probed with a high impedance buffer (U_{out}) which transfers the electric potential from C_m to the impedance of the measurement device such as an oscilloscope. An SPV signal arises practically immediately at C_m due to electrostatic induction (denoted by $U_{in\text{-}SPV}$ in the following).

The input capacitance and input resistance of an ideal high impedance buffer are zero and infinitely large, respectively. However, high impedance buffers are realized with electronic devices such as operational amplifiers (OPAs) that have a bias current (I_{bias}), an input capacitance (C_{in}), and an input resistance (R_{in}). The values of I_{bias}, C_{in}, and R_{in} have consequences for the SPV measurements.

First, the input capacitance acts together with C_m as a capacitive voltage divider which leads to a reduction of U_{out} to

$$U_{out} = U_{in} \cdot \frac{C_m}{C_m + C_{in}}. \quad (1)$$

For the analysis of the height of SPV signals, Equation (1) should be taken into account.

Second, the I_{bias} and R_{in} can be very high. For example, I_{bias} and R_{in} of the typical OPA656 are 2 pA and of the order of TΩs, respectively. For a very large product of I_{bias} and R_{in}, U_{in} is limited by the operation voltage of the high impedance buffer. For SPV measurements, the offset or bias potential of U_{in} ($\Delta U_{in\text{-}bias}$) has to be limited by a large shunt resistance, also called the measurement resistance (R_m) so that

$$\Delta U_{in-bias} = I_{bias} \cdot R_m. \quad (2)$$

For example, ΔU_{in} amounts to 2 mV for R_m and I_{bias} equal to 1 GΩ and 2 pA, respectively.

Third, C_m charges in time by I_{bias}. This results in a drift of U_{in} denoted by $U_{in\text{-}bias}$

$$\frac{dU_{in-bias}}{dt} = \frac{I_{bias}}{C_m}. \quad (3)$$

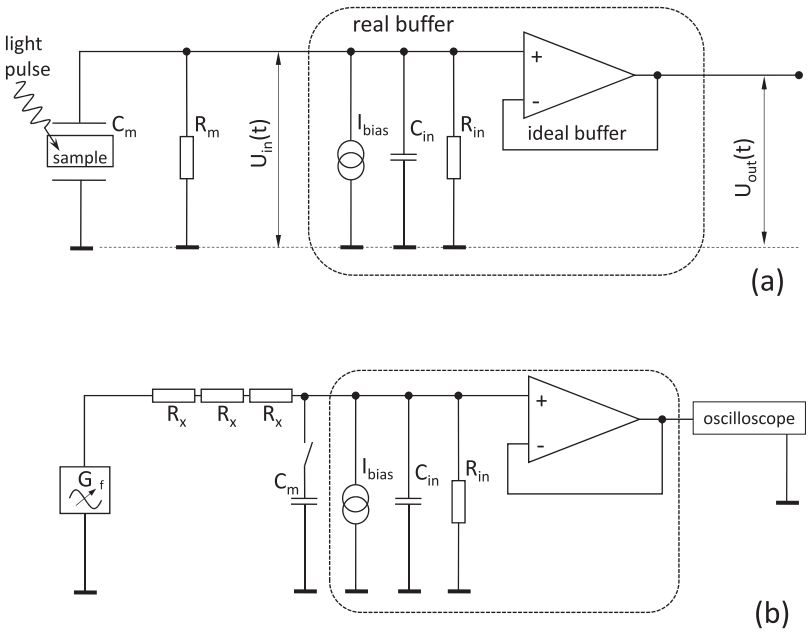

FIG. 2. Equivalent circuit of a high impedance buffer connected with the measurement capacitance (C_m) and measurement resistance (R_m) (a) and equivalent circuit for the measurement of the stray (C_{in}) and measurement capacitances with added resistances (R_x), a function generator, and an oscilloscope (b).

For example, at the beginning of charging, the drift is as high as 0.1 V/s for I_{bias} and C_m equal to 2 pA and 20 pF, respectively.

Fourth, C_m charges ($U_{in\text{-}bias}$) and discharges ($U_{in\text{-}SPV}$) via R_m with a time constant (τ_{RC})

$$\tau_{RC} = R_m \cdot C_m. \quad (4)$$

A typical value of τ_{RC} is, for example, 50 ms for R_m and C_m equal to 1 GΩ and 50 pF, respectively. $U_{in\text{-}SPV}$ lasting longer than τ_{RC} decays with τ_{RC}. On the other hand, $U_{in\text{-}SPV}$ decays with the characteristic time of the sample if this time is shorter than τ_{RC}, i.e., only processes resulting in relaxation of SPV signals shorter than τ_{RC} can be investigated. As a consequence, processes leading to a very long relaxation in relation to τ_{RC} or to an even permanent change of the CPD under illumination cannot be studied by SPV in the fixed capacitor arrangement.

For transient SPV measurements over a very long time range, a high impedance buffer and an oscilloscope with a wide frequency range and short light pulses are required together with a long τ_{RC}, i.e., high values of R_m and/or C_m. However, there is a tradeoff between a high value of R_m and I_{bias} due to the time-dependent increase of $U_{in\text{-}bias}$ and the time-dependent decrease of $U_{in\text{-}SPV}$.

For this work, we applied an OPA with an extremely low I_{bias} of the order of 3 fA (LTC6268). The extremely low I_{bias} allowed us to use the R_{in} of the OPA directly as the measurement resistance, i.e., R_m was equal to R_{in}. Under the assumption that $U_{in\text{-}bias}$ and $U_{in\text{-}SPV}$ can be treated independently, one gets the idealized time dependencies,

$$U_{in-bias}(t) = I_{bias} \cdot R_m \cdot \left(1 - \exp\left(-\frac{t}{R_m \cdot C_m}\right)\right), \quad (5)$$

$$U_{in-SPV}(t) = SPV(t) \cdot \exp\left(-\frac{t}{R_m \cdot C_m}\right). \quad (6)$$

Figure 3 illustrates the general behavior of $U_{in\text{-}bias}(t)$ and $U_{in\text{-}SPV}(t)$ for the high-impedance buffers based on the OPAs OPA656 (I_{bias} equal to 2 pA) and LTC6268 (I_{bias} equal to 2 fA). The values of R_m were chosen as 1 GΩ and 500 TΩ for the OPA656 and LTC6268, respectively. The value of C_m was set to 50 pF. Both buffers give identical transients for SPV signals with a short relaxation time such as 100 ns.

The relaxation of SPV signals over many orders of magnitude can often be described by stretched exponentials. As an example for a very long relaxation of a SPV signal, a stretching parameter (β) of 0.2 and a time constant (τ) of 10 s were chosen. Deviations between the bare stretched exponential and $U_{in\text{-}SPV}$ were obtained for times longer than about 30 ms or $3 \cdot 10^3$ s for the OPA656 or the LTC6268, respectively. However, due to the tradeoff mentioned before, deviations between the bare stretched exponential and the superposition of $U_{in\text{-}SPV}$ and $U_{in\text{-}bias}$ started for the LTC6268 already at times significantly shorter than 3000 s. Furthermore, this time becomes even shorter with decreasing height of the SPV signal. For shifting the time range to times longer than about 1000 s, C_m has to be increased, for example, by reducing the thickness of the insulator or by increasing the area of the electrode. The last one has consequences for SPV setups since homogeneous

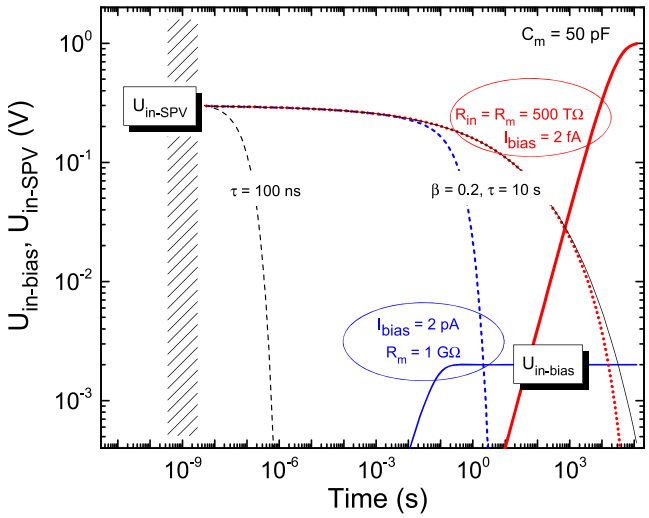

FIG. 3. Time dependencies of $U_{in\text{-}bias}$ (solid lines; after Equation (5)) for I_{bias} and R_m equal to 2 pA and 1 GΩ and to 2 fA and 500 TΩ (thin and thick lines, respectively; after Equation (6)) and of the corresponding $U_{in\text{-}SPV}$ (dashed lines and dotted line, respectively) for a stretched exponential with β and τ equal to 0.2 and 10 s, respectively. For comparison, the thin dashed and solid lines show an exponential decay with τ equal to 100 ns and a stretched exponential with β and τ equal to 0.2 and 10 s, respectively.

illumination over the whole area of the measurement capacitor is required.

A measurement capacitor can be formed, for example, by samples at floating potential between two insulators with the electrodes, by samples with a grounded back contact and a removable insulator on top with the front electrode (usually for the investigation of thin or extremely thin layers and of powders), or by samples with a back contact and an electrolyte front contact (Helmholtz-layer). The configuration of the measurement capacitor has strong influence on C_m. In this work, a sample with a well-defined grounded back contact and an insulator with the front electrode was applied.

III. EXPERIMENTAL

A glass substrate coated with conductive SnO_2:F was used as the back electrode onto which a photoactive nanoporous TiO_2/In_2S_3 double layer was deposited.[12] One advantage of the TiO_2/In_2S_3 double layer was that it contains a charge-selective interface at which photo generated electrons are separated relatively fast into the TiO_2. Furthermore, the density of trap states is high in the TiO_2/In_2S_3 double layer. This results in trap-limited transport and therefore in recombination of photo generated charge carriers separated in space over a long time. For the demonstration, the long relaxation time of SPV signals was limited to a range of the order of 100 s by setting the temperature of the sample to 65 °C.

For transients' SPV measurements, photo generated charge carriers were excited with single pulses of a tunable Nd:YAG laser (EKSPLA 341/1/UVE, duration time of a pulse about 5 ns, wavelength fixed at 535 nm, and intensity about 1 mJ/cm^2). For spectral dependent SPV measurements, illumination was performed with light of a halogen lamp (100 W) the wavelength of which was continuously changed with a quartz prism monochromator (SPM2) between 0.4 and 5 eV

within 1200 or 600 s. The light intensity was about 20 μW/cm^2 at 2 eV for the spectral dependent measurements. The SPV signals were measured with an oscilloscope (HP54510B, use of the sampling rate of 1 GS/s), with an oscilloscope card (GaGe CS14200, use of sampling rates between 100 MS/s and 100 kS/s), and with an multimeter (HP34401A, read out with a sampling rate of 2 S/s).

The SPV measurements were performed in a home-made vacuum chamber (pressure 10^{-3} Pa) with BNC-feedthroughs and a quartz window. For precise measurements at long times, ground loops had been avoided by insulating the vacuum chamber with electrical vacuum breaks against the vacuum pumps (rotary pump and turbomolecular pump) and by insulating the vacuum chamber against the optical table so that the chamber was only connected with the ground of the measurement device via the BNC-feedthrough.

Figure 4 shows a schematic of the electronic part for transient SPV measurements over 12 orders of magnitude in time in high vacuum. The fixed capacitor, also called the measurement capacitor, was formed between the sample electrode with an insulator (mica sheet, tens of μm thick) and a front electrode (see the inset in Figure 4). The sample electrode was grounded. The front electrode was made from a quartz cylinder (diameter 7 mm) covered with a transparent (or semitransparent) conductive oxide such a SnO_2:F at the side contacting the insulator.[13]

The high impedance buffer was connected with the measurement electrode by a cable as short as possible in order to reach a high resolution in time and in order to minimize the parasitic capacitance. For this purpose, the high impedance buffer was realized with small SMD ceramic based capacitors which allowed to place the high impedance buffer directly into the high vacuum chamber. The resistance at the output of the high impedance buffer was 50 Ω. In addition, the input of the high impedance buffer was connected with a resistance of 1 GΩ in series via a Reed contact for resetting the charge at the measurement capacitor from time to time. The Reed contact was switched with a coil of copper wire (reset current of 300 mA) that was directly wound onto the glass tube of the Reed contact in order to minimize parasitic capacitances and resistances.

The output signal from the high impedance buffer was transferred from the high vacuum chamber to the preamplifier via the BNC-feedthrough. In the preamplifier, the signal was amplified by a factor of 2. The same shielded box provided the electric power for the buffer and for the amplifier. The outputs from the amplifier (50 Ω and 1 kΩ) were connected with an oscilloscope (output with 50 Ω) and with a multimeter (output with 1 kΩ).

The values of C_{in} and C_m were measured with a frequency generator, an oscilloscope, and added resistances (Figure 2(b)). For this purpose, three resistances (R_x) were connected as close as possible to the high impedance buffer. This was done so to reduce the parasitic capacitance of each single resistance (about 0.2 pF for the given configuration type 0207). The frequency at which the signal decreased by $2^{-0.5}$ times in comparison to the value at low frequencies was obtained (f_{3dB}, which was the reciprocal RC time constant). As a remark, the corresponding resolution time is equal to the RC time constant divided by $2 \cdot \pi$. The C_{in} was calculated by the following equation:

$$C_{in} = \frac{1}{2\pi \cdot 3R_x \cdot f_{3dB}}. \tag{7}$$

In the setup used for the given experiments, f_{3dB} amounted to 15.8 kHz for an R_x of 1 MΩ resulting in a C_{in} of 3 pF. The value of C_m has been found in a similar way. As a remark, C_m can vary over a relatively wide range depending on the thickness of the insulator, on the material of the insulator, and on the sample (C_m between 7 and 100 pF for related set-ups). For the given experimental setup, a parasitic capacitance including, for example, the influence of the grounded heater was not distinguished from C_{in}. Furthermore, the charging behaviors of C_{in} and C_m by I_{bias} were measured up to times longer than $2 \cdot 10^4$ s and fitted with Equation (5) whereas a time shift and a starting value were considered due to possible pre-charging. From these fits, values of R_{in} and I_{bias} of 700 ± 100 TΩ and 1.1 ± 0.3 fA, respectively, were obtained for the used OPA LTC6268.

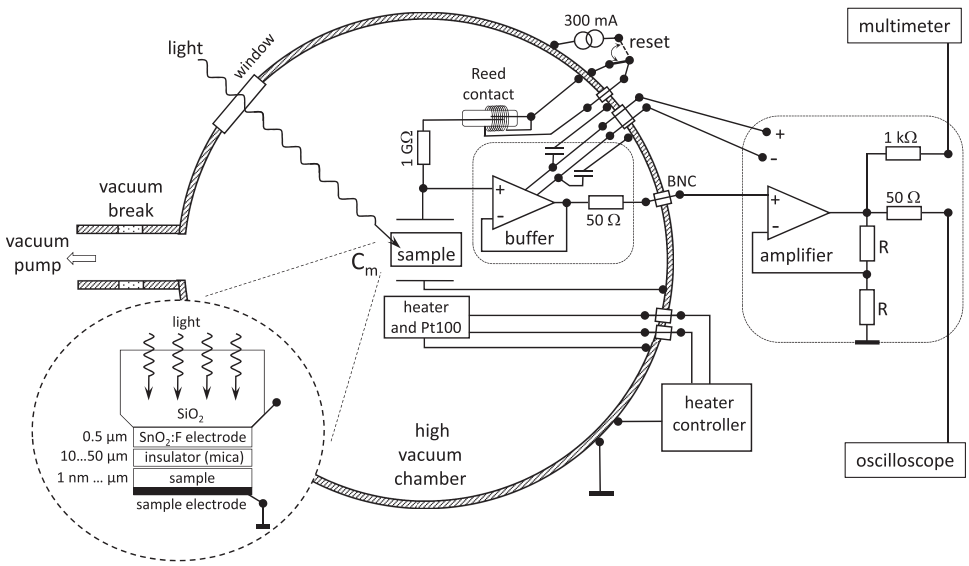

FIG. 4. Schematic of the electronic part for transient surface photovoltage measurements over 12 orders of magnitude in time in high vacuum. The inset gives the structure of the measurement capacitor. The thickness of the insulator (mica sheet) is much larger than the relevant thickness of the sample.

IV. RESULTS AND DISCUSSION

Figure 5 shows consecutive SPV transients measured with different sampling rates. For the sampling rate of 100 MS/s, the first SPV transient had an offset of −31 mV, set on within the first 10 ns after the laser pulse was switched on (set to 6 ns) and reached at 760 ns a maximum of 246 mV, i.e., the SPV amplitude was 277 mV. For the 2nd and 5th SPV transients, which followed 100 s after the 1st and 4th SPV transients, respectively, the offsets increased to −45 and −70 mV and maxima of 236 and 209 mV were reached at 750 and 650 ns, respectively. The sign of the SPV signals was positive. This means that photo-generated electrons were separated towards the bulk of the sample. The maximum was reached after a time much longer than the duration time of the laser pulse. This behavior can be interpreted as an increase of the charge separation length with increasing time due to diffusion of electrons injected into TiO_2. This phenomenon is also known, for example, from transient SPV measurements on nanoporous silicon,[14,15] poly(*p*-phenylenevinylene),[16] or TiO_2.[17]

The change in the onsets was simultaneously monitored with the multimeter readout (sampling rate of 2 S/s). Slight changes in the SPV amplitude were probably caused by fluctuations in the intensity of the laser pulses whereas changes of the time at maximum towards shorter times gave evidence for faster relaxation of photo-generated charge carriers with consecutive illumination. This is caused by filling of deep trap states which do not discharge within consecutive SPV transients. Therefore, the change of the offset of the consecutive SPV transients was caused not only by drift due to I_{bias} but also by discharging of traps. In this sense, it is not straightforward to define a baseline for consecutive transients.

Figure 6 gives an example for the drift of the potential over several thousands of seconds before and after one laser pulse. The buffer was stabilized within a few hundred seconds. As a remark, the time dependence could be fitted with Equation (5) at times shorter than the laser pulse. However, the fit of the drift could much better fitted with a stretched exponential,

$$U = U_0 \cdot \exp\left[-\left(\frac{t - t_0}{\tau}\right)^{\beta}\right] - U_1. \quad (8)$$

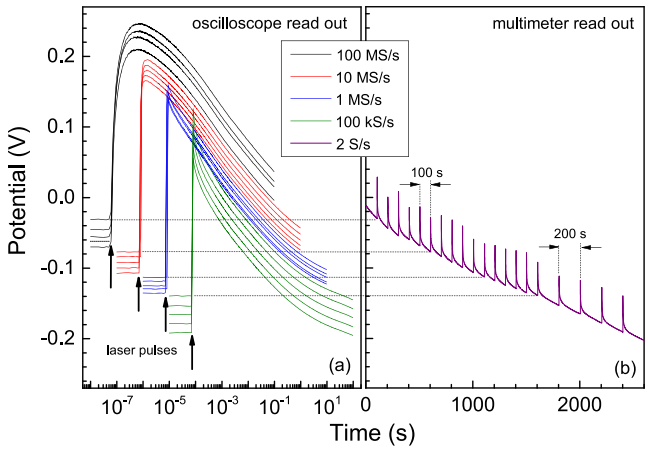

FIG. 5. Consecutive surface photovoltage transients measured with the sampling rate of 100 Ms/s, 10 Ms/s, 100 kS/s (a), and 2 S/s (b) (black, red, blue, green, and pink lines, respectively). The arrows mark the onset times of the laser pulse. The drift of the baseline in time can be clearly seen.

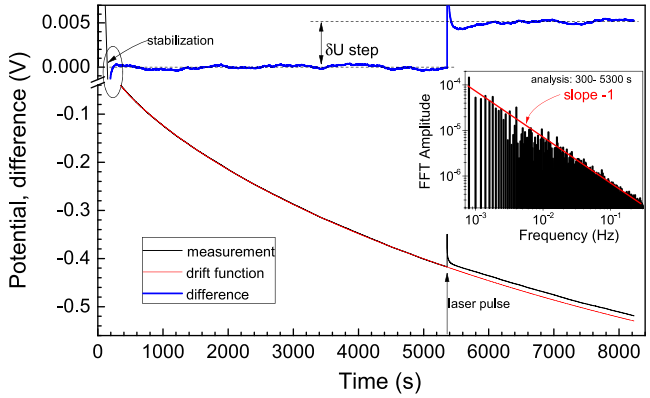

FIG. 6. Example for the drift of the potential over several thousands of seconds before and after one laser pulse (black line), stretched exponential fit function of the measurement (fitted in the range between 300 and 5300 s, red line), difference between the measurement and the stretched exponential (blue line), and frequency spectrum of the difference between the measurement and the stretched exponential (from FFT in the range between 300 and 5300 s, inset).

For the fit in the range between 300 and 5300 s, the values of t_0 and of the potentials U_0 and U_1 amounted to 190 s and 0.9196 and 0.9265 V, respectively. The time constant (τ) and the stretching parameter (β) were 10^4 s and 0.8, respectively. The standard deviation of the difference between the measured potential and the fit function was 0.2 mV. As a remark, a set of parameters of a stretched exponential could be obtained as one common drift or baseline for any sample, i.e., the nature of a sample and its history can play an important role for SPV measurements at long time.

The difference between the measured potential and the fit function is also shown in Figure 5. The sample was illuminated with the laser pulse at 5360 s. The difference between the measured potential and the fit function was a straight line in the regions between 300 and 5360 s and between about 6000 and 8200 s, when the measurement was finished. There was a step of 5 mV between both regions, i.e., the laser pulse induced a change of fixed (within the measurement time) charge at the sample surface. Furthermore, the step of 5 mV was undershoot by up to 1 mV in the region between 6000 and 5800 s. This undershoot gave evidence for separation of photo-generated charge carriers with opposite direction and very different relaxation times. The step and undershoot of the signal can be reduced by increasing the repetition rate of the laser pulses to the order of 1 Hz, which is a common frequency for transient SPV measurement, and by averaging over many pulses. The Fast Fourier Transform analysis of the difference between the measured potential and the fit function resulted in a 1/f frequency dependence (see the inset of Figure 6).

A drift correction can be introduced if limiting the time interval of consecutive transients, for example, to 1000 s. In the following, we defined the drift as the linear function defined by the SPV signals just before consecutive laser pulses. Obviously, the SPV transients measured at high sampling rates are practically not affected whereas the experimental error may become significant at long time. The measurement of transient SPV signals over 12 orders of magnitude could not be realized with only one sampling rate and one transient. Figure 7 gives an example for a SPV transient which has been

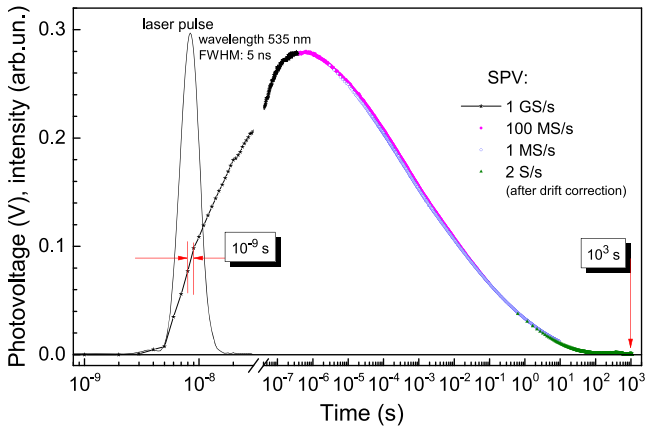

FIG. 7. Example for a surface photovoltage transient over 12 orders of magnitude in time made up of four transients measured with the sampling rate of 1 Gs/s, 100 Ms/s, 1 Ms/s, and 2 S/s (black stars, red filled circles, blue open circles, and green triangles, respectively). The thin solid line gives the shape of the laser pulse.

measured between 1 ns and 1000 s. Four consecutive transients were measured in the order of the sampling rates of 100 MS/s, 1 MS/s, 2 S/s, and 1 GS/s and with a relatively wide overlap in time. The transients did not perfectly coincide (the first one was the slowest as already mentioned) due to trap filling. The strongest increase of the SPV signal was found during the increase of the laser pulse within about 4 ns. The intensity of the laser pulse almost started to increase about 2 ns before the main pulse. This behavior was also found in the SPV transient. The SPV transient decayed over about 8 orders of magnitude and leveled out within about 100 s.

In SPS measurements with a Kelvin probe, a sample is continuously illuminated with light the photon energy of which is increasing in time. With a high impedance buffer, similar measurements can be performed if I_{bias} is very low so that a measurement can be performed over hundreds or thousands of seconds. Figure 8 shows a sequence in time during four measurements of the spectral dependent potential. The time interval was reduced by reducing the number of averages per wavelength from 10 to 2. All signals changed in a similar way along an approximate baseline.

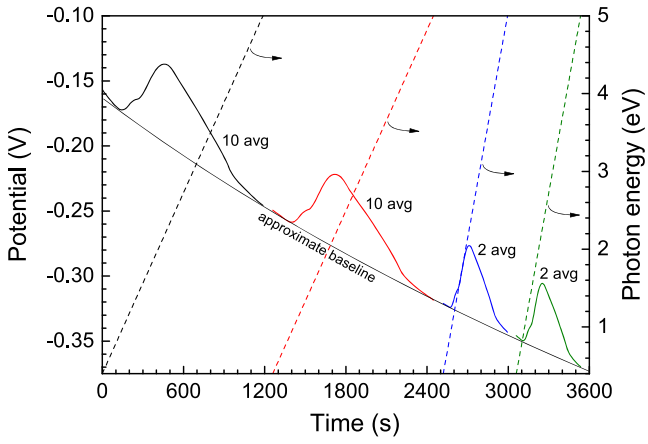

FIG. 8. Sequence in time of the spectral dependent potential (four consecutive scans, sampling rate 2 S/s) averaged 10 times (black and red parts) and 2 times (blue and green parts). The dashed lines mark the corresponding photon energies in time. The thin black line gives an overall approximate baseline.

The sequence in time shown in Figure 9 has been converted into four spectra (Figure 9(a)). A baseline can be defined from the part of the spectrum in which SPV signals are still absent. However, such a baseline is only reliable for the spectral range with low photon energies when the SPV signals are still low. An approximate baseline is shown for the fourth scan. The difference between the spectrum of the potential and the baseline gives an SPV spectrum. The SPV spectrum of the fourth scan is shown in Figure 9(b) in a semi-logarithmic plot. As a remark, SPV signals do not necessarily correlate linearly with the photon flux. Therefore, a normalization to the photon flux was not done.

Defects with transitions near the band edges lead to so-called exponential tails in absorption spectra. In spectral dependent SPV measurements, a related energy describing an exponential tail can also be obtained. However, one has to keep in mind that the measured values of tail energies (E_t) can depend on the method and on the measurement conditions due to the influence of transport related phenomena. For the investigated sample, the SPV signal increased exponentially over more than 20 times in the range between 0.75 and 1.05 eV. At the same time, the light intensity changed by only 40% in the given spectral range. The value of E_t amounted to about 0.1 eV This relatively high value of E_t gives evidence for disorder in the sample and can explain the long relaxation of the SPV transients due to hopping and distant dependent recombination. Recently, we showed on a monolayer of quantum dots that SPV transients can be fitted with random walks[18] whereas parameters of defects could be extracted. However, to date, the given system is still too big for fitting of transients.

The pronounced shoulder in the spectrum (Figure 9(b)) around 1.5 eV was caused by the change in the spectrum of the photon flux. The SPV signal did not decrease to zero at high photon energies (above 3.5 eV) despite the fact that the

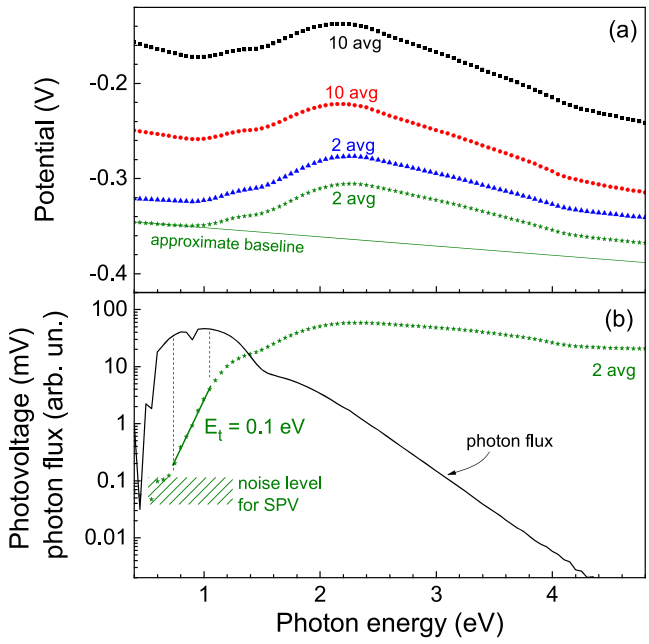

FIG. 9. Potential spectra deduced from Figure 7 (symbols) and approximate baseline for the fourth scan (2 averages, line) (a) and surface photovoltage spectrum for the fourth scan (symbols) and spectrum of the photon flux (line) (b).

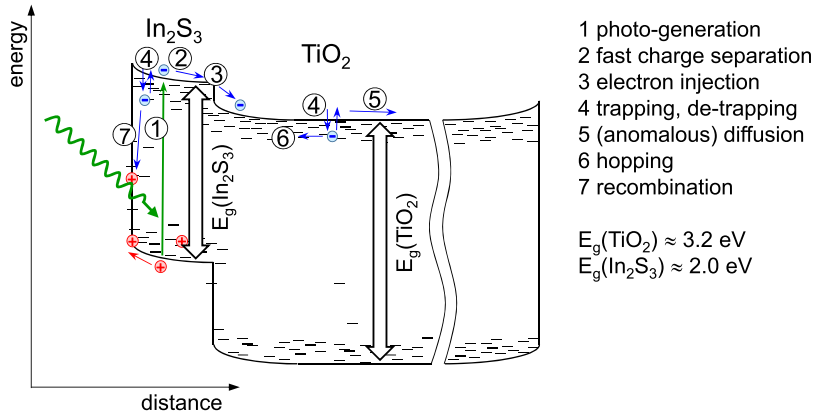

FIG. 10. Illustration of processes in an In_2S_3/TiO_2 layer system. Fast charge separation takes place in the built-in electric field. Trapping, de-trapping, and hopping lead to retarded charge separation and long lasting relaxation until distant dependent recombination.

photon flux almost decreased to very low values. The reason for this is the slow discharge of deep traps. As a consequence, one has to be careful with the interpretation of features in the spectrum appearing in the ultraviolet range.

Figure 10 illustrates processes in an In_2S_3/TiO_2 layer system. The bandgaps of In_2S_3 and TiO_2 are indicated. The band-offsets are not well known and depend sensitively on the processing.[11] The tail states measured are related to absorption in the In_2S_3 layer. In the built-in electric field, charge carriers photo-generated from localized or delocalized states into extended states can be separated within the duration of the laser pulse due to drift (fast charge separation due to drift). In the following, electrons are getting trapped and de-trapped that leads to trap-limited and/or hopping transport. This causes a retarded charge separation in space and long lasting relaxation until distant dependent recombination takes place. Therefore, related processes can be studied by time dependent SPV.

V. CONCLUSIONS

The measurement of SPV signals in the fixed capacitor arrangement over 12 orders of magnitude in time and of non-modulated SPV spectra has been demonstrated for a high impedance buffer with extremely low bias current. The noise of the SPV signals was limited by the 1/f noise of the high impedance buffer. The huge dynamic range of SPV measurements in the fixed capacitor arrangement is unique in comparison to all the other ways to detect SPV signals.

The resolution in time can be further improved if using laser pulses shorter than 1 ns and oscilloscopes with sampling rates higher than 1 GS/s. The influence of charging/discharging phenomena on one transient can be eliminated if triggering at the same time two oscilloscope cards with very large memory set to different sampling rates and one multimeter for monitoring changes in long time.

The increased dynamic range of SPV measurements in the fixed capacitor arrangement was demonstrated on the example of fast charge separation and transport limitation by traps in an In_2S_3/TiO_2 system. The possibility to measure SPV signals over 12 orders of magnitude in time opens new opportunities to the combined investigation of processes of charge separation related to fast electronic processes, dispersive transport or tunneling limited recombination, photo-induced ionic transport, and charging/discharging of adsorbates. Furthermore, the increased dynamic range can also give inspiration to the further development of related techniques such as deep level transient spectroscopy in comparison to SPV.[19]

[1] See, for example, L. Kronik and Y. Shapira, Surf. Sci. Rep. **37**, 1 (1999).
[2] K. Besocke and S. Berger, Rev. Sci. Instrum. **47**, 840 (1976).
[3] M. Nonnenmacher, M. P. O'Boyle, and H. K. Wickramasinghe, Appl. Phys. Lett. **58**, 2921 (1991).
[4] F. Streicher, S. Sadewasser, and M. Ch. Lux-Steiner, Rev. Sci. Instrum. **80**, 013907 (2009).
[5] F. Steinrisser and R. E. Hetrick, Rev. Sci. Instrum. **42**, 304 (1971).
[6] J. Clabes and M. Henzler, Phys. Rev. B **21**, 625 (1980).
[7] M. Ogawa, S. Yamamoto, R. Yukawa, R. Hobara, C.-H. Lin, R.-Y. Liu, S.-J. Tang, and I. Matsuda, Phys. Rev. B **87**, 235308 (2013).
[8] A. Shavorskiy *et al.*, Rev. Sci. Instrum. **85**, 093102 (2014).
[9] B. F. Spencer *et al.*, Phys. Rev. B **88**, 195301 (2013).
[10] E. O. Johnson, J. Appl. Phys. **28**, 1349 (1957).
[11] Th. Dittrich, S. Bönisch, P. Zabel, and S. Dube, Rev. Sci. Instrum. **79**, 113903 (2008).
[12] A. O. Juma, A. Azarpira, A. Steigert, M. Pomaska, C.-H. Fischer, I. Lauermann, and Th. Dittrich, J. Appl. Phys. **114**, 053711 (2013).
[13] V. Duzhko, V. Yu. Timoshenko, F. Koch, and Th. Dittrich, Phys. Rev. B **64**, 075204 (2001).
[14] V. Duzhko, F. Koch, and Th. Dittrich, J. Appl. Phys. **91**, 9432 (2002).
[15] Th. Dittrich and V. Duzhko, Phys. Status Solidi A **197**, 107 (2003).
[16] V. Duzhko, Th. Dittrich, B. Kamenev, V. Yu. Timoshenko, and W. Brütting, J. Appl. Phys. **89**, 4410 (2001).
[17] Th. Dittrich, I. Mora-Seró, G. Garcia-Belmonte, and J. Bisquert, Phys. Rev. B **73**, 045407 (2006).
[18] S. Fengler, E. Zillner, and Th. Dittrich, J. Phys. Chem. C **117**, 6462 (2013).
[19] J. Lagowski, A. Morawski, and P. Edelman, Jpn. J. Appl. Phys., Part 2 **31**, L1185 (1992).